GLIA 58:66–79 (2010)

Axons and Astrocytes Release ATP and Glutamate to Evoke Calcium Signals in NG2-Glia

NICOLA HAMILTON, STEVE VAYRO, REBEKAH WIGLEY, AND ARTHUR M. BUTT*
Institute of Biology and Biomedical Sciences, School of Pharmacy and Biomedical Sciences, University of Portsmouth, United Kingdom

KEY WORDS
NG2; synantocyte; glia; oligodendrocyte precursor; OPC; astrocyte; ATP; glutamate; axon

ABSTRACT
NG2-glia are an abundant population of cells in the adult CNS that make up a novel glial cell type. Here, we have examined calcium signals in NG2-glia identified by expression of the fluorescent protein DsRed under the control of the NG2 promoter in the white matter of the mouse optic nerve. We focused on mice aged postnatal day (P)12–16, after the main period of oligodendrocyte generation. Using fluo-4 and fura-2 calcium imaging in isolated intact nerves, we show that glutamate and ATP evoke Ca^{2+} signals in NG2-glia *in situ*, acting on AMPA-type glutamate receptors and $P2Y_1$ and $P2X_7$ purine receptors; NMDA evoked a weak Ca^{2+} signal in a small proportion of NG2-glia. We show that axonal action potentials and mechanical stimulation of astrocytes effect the release of glutamate and ATP to act on NG2-glia; ATP alone evokes robust Ca^{2+} signals, whereas glutamate did not unless AMPA receptor desensitization was blocked with cyclothiazide. We identify the precise contacts that NG2-glia form with axons at nodes of Ranvier, and the intricate bipartite sheaths formed between the processes of NG2-glia and astrocytes. In addition, we provide evidence that NG2-glia express synaptophysin, indicating they have mechanisms for transmitting as well as receiving signals. This study places NG2-glia within a neuron-glial network, and identifies roles for glutamate and ATP in communication with astrocytes as well as axons.

INTRODUCTION

Calcium excitability is the mechanism of intercellular signaling between astroglia in response to neurotransmitters released at synapses (Verkhratsky et al., 1998). Moreover, astroglia release the "gliotransmitter" adenosine triphosphate (ATP) to propagate an intercellular calcium wave between astrocytes (Coco et al., 2003; Newman, 2001). Recently, a population of novel NG2-expressing glia have also been shown to respond to glutamate released along axons in white matter (Kukley et al., 2007; Ziskin et al., 2007). Notably, white matter astrocytes also release neurotransmitters to propagate intercellular Ca^{2+} signals to neighboring glia (Hamilton et al., 2008). In addition, we have recently provided evidence that glutamate and ATP evoke increased intracellular Ca^{2+} in NG2-glia in the rat optic nerve (Hamilton et al., 2009). These studies raised the possibility that both axons and astrocytes may release neurotransmitters to evoke Ca^{2+} signals in NG2-glia.

NG2-glia are a substantial population of cells in the CNS, which we have argued are a novel glial cell type termed synantocytes (Butt et al., 2002, 2005). There is some confusion in the literature about the nature of these cells, and so in this article we will refer to them simply as NG2-glia. Two distinguishing features of these cells is their expression of the NG2 chondroitin sulphate proteoglycan (CSPG) and platelet-derived growth factor alpha receptors (PDGFαR). These are markers of oligodendrocyte progenitor cells (OPCs), and genetic fate tracing in double transgenic mice shows oligodendrocytes are generated from NG2/PDFGαR-glia in the developing and mature CNS (Rivers et al., 2008; Zhu et al., 2008). However, NG2-glia may have functions in addition to serving as a pool of OPCs in the mature CNS (Butt et al., 2005). For example, in the molecular layer of the cerebellum, which is devoid of oligodendrocytes, NG2-glia receive synaptic input from rising fibers and respond to synaptically released glutamate (Lin et al., 2005). The functions of neuron-NG2-glial signaling are unresolved, but they place NG2-glia firmly within the cerebellar neuron-glial network (Wigley et al., 2007). In white matter, NG2-glia contact myelinated axons at nodes of Ranvier, the sites of axonal action potential propagation (Butt et al., 1999), which have now been shown to be sites of synaptic glutamate release (Alix et al., 2008). Axonal activity in the optic nerve has been known for some time to evoke Ca^{2+} signals in glia (Kriegler and Chiu, 1993), and we have identified a key role for ATP in astroglial Ca^{2+} signaling (Hamilton et al., 2008). Here, we make use of mice in which expression of DsRed is under the control of the NG2 promoter (Zhu et al., 2008) to show that glutamate and ATP released during axonal action potential propa-

Nicola Hamilton and Steve Vayro contributed equally to this article.

Nicola Hamilton is currently at Department of Physiology, University College London, United Kingdom.

Grant sponsors: BBSRC and Anatomical Society PhD studentship (to N.H.).

*Correspondence to: Arthur Butt, School of Pharmacy and Biomedical Sciences, University of Portsmouth, St Michael's Building, White Swan Road, Portsmouth PO1 2DT, United Kingdom. E-mail: arthur.Butt@port.ac.uk

Received 22 February 2009; Accepted 8 May 2009

DOI 10.1002/glia.20902

Published online 16 June 2009 in Wiley InterScience (www.interscience.wiley.com).

gation and mechanical stimulation of astrocytes evoke Ca^{2+} signals in NG2-glia.

MATERIALS AND METHODS

Animals and Tissue

Experiments were performed on optic nerves and cerebral cortex from NG2-DsRed BAC transgenic mice, a gift from Dr. Akiko Nishiyama (Corrs University, USA), in which DsRed (drFP583, from Discosoma species) is co-expressed with the NG2 CSPG (Ziskin et al., 2007; Zhu et al., 2008), and the *TgN*(*GFAPEGFP*)*GFEC-FKi* transgenic mouse line, a gift from Dr. Frank Kirchhoff (Goettingen University, Germany), in which glial fibrillary acidic protein (GFAP) drives expression of green fluorescent protein (GFP) in astrocytes (Nolte et al., 2001). In some cases, rat anterior medullary velum were used for immunohistochemistry, as described previously (Butt et al., 1999). Animals aged postnatal day (P)12–16 of either sex were killed humanely by lethal intraperitoneal injection of sodium pentobarbitone or cervical dislocation, in accordance with regulations issued by the Home Office of the United Kingdom under the Animals (Scientific Procedures) Act, 1986.

Calcium Imaging

Calcium imaging was performed on optic nerves from NG2-DsRed mice. Optic nerves were removed intact and placed immediately in ice-cold oxygenated artificial cerebrospinal fluid (aCSF, mM: NaCl, 133; KCl, 3; $CaCl_2$, 1.5; NaH_2PO_4, 1.2; $MgCl_2$, 1.0; D-glucose. 10; HEPES, 10; pH 7.3). The arachnoid membrane was carefully removed and nerves were incubated for 1 h at room temperature (RT) in oxygenated aCSF containing either Fura-2 AM or Fluo-4 (4 μM; molecular probes). Dye-loaded nerves were then placed in a chamber on an upright microscope and perfused continuously with aCSF. Fluo-4 loaded nerves were visualized using a 20×/0.50 WPh2 Achroplan water immersion lens on a Zeiss LSM 5 Pascal Axioskop 2 confocal microscope. Nerves were excited at 543 nm for NG2/DsRed and at 488 nm for fluo-4, and images were collected at 3 Hz in optical z-sections (typically <10 slices at 2–3 μm intervals, using a pinhole of ≤0.9). Cell bodies within a single z-section were selected as regions of interest (ROI) and the change in fluorescence intensity was measured using Zeiss LSM Image Examiner software V 4.0 (Carl Zeiss, Germany). For fura-2, nerves were visualized using an Achroplan 20× water immersion lens (with an optional 2× multiplier) on an Olympus upright epifluorescence microscope (BX50W1). DsRed-positive NG2-glia were first identified at 543 nm excitation and 585 nm emission and cell bodies within a single plane of focus were selected as ROI. Fura-2 was excited alternately at 340 and 380 nm, using a Cairn monochromator (Cairn Research Ltd, UK), and emissions were detected at 510 nm using an intensified CCD camera or a Photometrics S-Coolsnap CCD camera (both supplied by Cairn Research, UK). The monochromator and the CCD camera were controlled and synchronized by Axon Imaging Workbench 5.1 (Axon Instruments), and quantitative measurements were made using the same program. Signals were sampled at 2 Hz and in the selected ROI the change in *F*340:*F*380 ratio was measured relative to the baseline fluorescence after background subtraction (Δ*F*340:*F*380).

Solutions and Application of Test Agents

All chemicals were from Tocris (Bioscience, Bristol, UK) or Sigma-Aldrych (Dorset, UK), and were dissolved directly in aCSF: adenosine 5′-triphosphate (ATP, Sigma); 2-methylthioadenosine triphosphate tetrasodium salt (2MeSATP, Tocris); 2′-3′-0-(4-benzoylbenzoyl) adenosine 5′-triphosphate (BzATP, Sigma); suramin hexasodium salt (suramin, Tocris); adenosine 5′-triphosphate-2′,3′-dialdehyde (oxidised ATP/oATP, Tocris); 2′-deoxy-*N*6-methyladenosine3′,5′-biphosphate, tetra ammonium salt (MRS2179, Tocris); L-glutamic acid (glutamate/Glu, Tocris); Cyclothiazide (CTZ, Tocris); *N*-methyl-D-aspartic acid (NMDA, Tocris); D-(−)-2-amino-5-phosphonopentanoic acid (D-AP5, Tocris); DL-threo-β-benzyloxyaspartate (TBOA, Tocris); 2,3-dioxo-6-nitro-1,2,3,4-tetrahydrobenzol[f]quinoxaline-7-sulfonamide disodium salt (NBQX, Tocris); DL-threo-β-benzyloxyaspartic acid (TBOA, Tocris). Agonists were applied for 30 s, unless otherwise stated, and a recovery period of 10 min in aCSF was allowed after each agent. Antagonists were applied for 3–5 min to ensure complete diffusion into the nerve.

Electrical Stimulation

Optic nerves were electrically stimulated to propagate axonal action potentials, as described previously (Bolton and Butt, 2005). One end of the nerve was taken up into a glass capillary filled with aCSF and connected via a Ag/AgCl wire to a S44 Grass stimulator (Grass Instruments); the circuit was completed by a second Ag/AgCl wire in contact with the bath solution. Stimulus strength was increased gradually to obtain the threshold at which cells were observed to respond with raised $[Ca^{2+}]_i$, and for recording purposes this stimulus strength was then applied at 20 Hz for 10 s, allowing 10 min recovery between stimuli. Each nerve could be stimulated in this way many times to evoke reproducible glial Ca^{2+} signals. Generally, two or three control stimuli in aCSF were followed by one or more stimuli in the presence of test agent, and then further stimuli following washout of the antagonist.

Mechanical Stimulation

Optic nerves were mechanically stimulated with a microelectrode using an established protocol (Hamilton et al., 2008; Newman, 2001). In brief, a glass micropip-

ette was mounted on a micromanipulator and the micropipette tip was placed directly above a large DsRed-negative fura-loaded cell, presumed to be an astrocyte. The microelectrode was advanced and retracted rapidly to mechanically stimulate the cell. A 10-min recovery period was allowed between stimuli, and cells could be stimulated in this way multiple times to evoke reproducible glial Ca^{2+} signals. Generally, two or three control stimuli in aCSF were followed by one or more stimuli in the presence of test agent, and then further stimuli following washout of the antagonist.

Data Analysis

Paired responses were made in each cell: for agonists, the peak response to a test agonist was expressed as a percentage of the response to 100 μM ATP or 100 μM glutamate in the same cell (denoted % ATP response, or % glutamate response); for antagonists, the response of the agonist in the presence of the antagonist was expressed as a percentage of the agonist response in the same cell; for electrical and mechanical stimulation, responses in the present of test agent were expressed as a percentage of the control response in aCSF in the same cell. Measurements were made from multiple cells (ROI) in each nerve and experiments were replicated in three to five nerves, data were then expressed as mean ± SEM, where *n* represents the number of cells, and tested for significance using analysis of variance (ANOVA) followed by a Bonferroni *t*-test, Mann-Whitney test, or unpaired Student's *t*-test, where appropriate.

Immunohistochemistry

Immunohistochemistry was performed on optic nerves and forebrain from NG2-DsRed and GFAP-EGFP mice aged P15, and anterior medullary vela from rats aged P12. Tissues were dissected free and immersion fixed in 4% paraformaldehyde at 4°C overnight, and in the case of brains and optic nerves vibratome sections were cut at 100 μm; vela were kept intact throughout. Following washes in PBS, a blocking stage was performed by incubation for 1 h at RT in 10% normal goat serum (NGS) and 0.3% triton-X-100 in phosphate buffered saline (PBST). After blocking, tissues were incubated overnight at 4°C with primary antibodies diluted in GS-PBS: rabbit anti-NG2 (1:500, gift from Dr. Stallcup; or 1:200, Chemicon); chicken anti-GFAP (1:200; Chemicon); rabbit anti-synaptophysin, (1:300 Chemicon); mouse anti-MBP (1:10, Serotec); rabbit anti-NF200 (1:500, Sigma Aldrych); rabbit anti-GluR4 (1:300, Chemicon); rabbit ant-NR2AC (1:300, Chemicon); chicken anti-AnkyrinG (1:500, gift from Dr. Stephen Lambert). After washes in PBS, tissues were incubated for 1 h at RT with the appropriate secondary antibodies conjugated with ^{488}Alexafluor, ^{567}Alexafluor, or ^{405}Alexafluor (1:500, molecular probes). Primary antibodies of different origin were diluted together in blocking buffer and co-dilutions of the appropriate secondary antibodies were used. Control experiments were carried out in which the primary antibody was omitted. After final washes in PBS, tissues were mounted on polylysine-coated glass slides with Vectashield mounting media (Vector Laboratories), and images were acquired using an LSM 5 Pascal Axioskop2 or LSM 510 meta confocal microscope (Zeiss). Fluorescence was visualized at 488 nm (green), 568 nm (red), and 405 nm (blue) using an argon, HeNe1, and diode lasers, respectively, using a 40× oil immersion lens with high numerical aperture (1.3 nm).

Image Analysis

Image visualization and analysis was carried out using Volocity software (Improvision, Perkin Elmer, UK). Image acquisition of the different laser lines was performed using multichannel sequential scanning and minimal laser power and gain to remove bleed between the channels. A pinhole of 1 airy unit or less was used, with an average of four scans per image. The number of z-sections and resolution were optimized using the Zeiss acquisition software, and in general z-sections were $\leq$0.75 μm thickness, and approximately 30 z-sections were taken for each cell. For confocal photomicrographs, two-dimensional flattened images of the z-stacks are presented. In some cases, isosurface rendering of images is used to illustrate equalized intensity of all pixels to provide three-dimensional representation. For colocalization analyses, all measurements were made of voxels in three dimensions. First, scatter graphs were plotted of voxel intensities of one channel against the intensity of the corresponding voxels in the other channel. Then, a colocalization channel was generated by selecting a region of interest (ROI) on the scatter-plot in the region where the voxels from the two channels overlap with the same intensity. The colocalization channel illustrates the true extent of colocalization of the two channels in three-dimensions. The Volocity software calculates a range of parameters, and we used the overlap coefficient according to Manders, which indicates the actual overlap of the signals from the two channels throughout the three-dimensional image (for further details of the coefficients see Zinchuk et al., 2007). The value for the overlap coefficient ranges from 0 to 1, where 0 is no colocalization and 1 is complete colocalization. In our analyses, an overlap coefficient of $\geq$0.5 indicated true colocalization. In this way, we analyzed the extent of colocalization between DsRed (568 nm) and the fluorochrome (488 nm), and mean overlap coefficients (±SEM) were calculated and tested for significance using unpaired *t*-tests.

RESULTS

Glutamate and ATP Stimulate Ca^{2+} Signals in NG2-Glia Within White Matter

Calcium imaging was performed in situ on P12–16 optic nerves from a transgenic mouse line in which

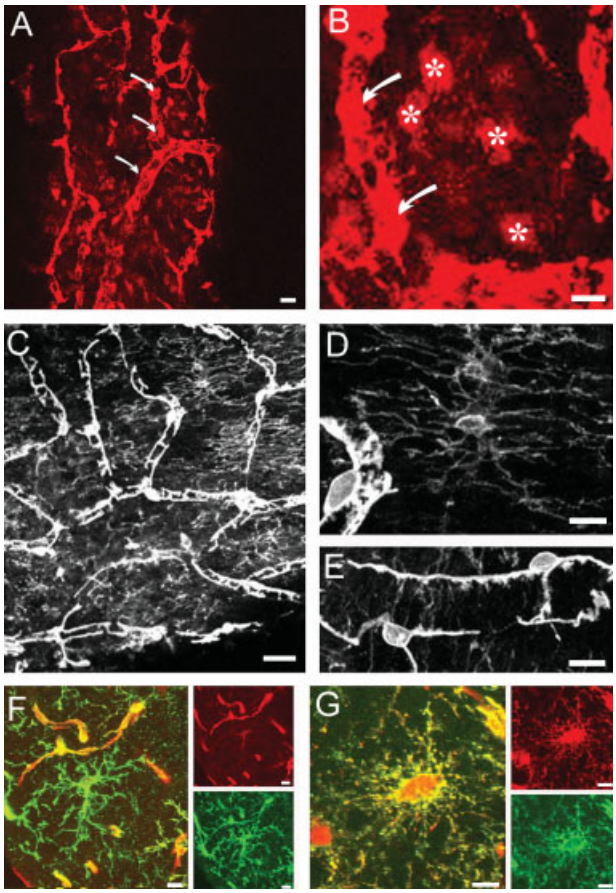

Fig. 1. Morphological features of NG2-glia and pericytes. Both NG2-glia and pericytes express the NG2 chondroitin sulphate proteoglycan, as illustrated in optic nerves isolated intact and alive from NG2-DsRed BAC mice (**A**, **B**), by immunolabeling for NG2 in optic nerve sections (**C**–**E**), and immunolabeling for NG2 in sections of brain from NG2-DsRed BAC mice (**F**, **G**). NG2-glia and pericytes are readily distinguished by their morphology and location within the nerve. (A) Pericytes are perivascular and at low magnification they identify the microvessels that supply the optic nerve. (B) In live optic nerves used for calcium imaging, which have not been fixed or cleared, pericytes are identified by their perivascular location and large soma directly apposed to blood vessels (curved arrows), whereas NG2-glia are identified by their small irregular somata, located away from blood vessels and fine processes (asterisks). (C–E) Immunolabeling for NG2 in fixed and cleared optic nerve sections illustrates the fine detail of the distinct morphological differences between pericytes and NG2-glia, the latter with extensive fine branching processes terminating up to 50 μm from the cell body. (F, G) Immunolabeling for NG2 in brain sections of NG2-DsRed BAC mice confirms coexpression of NG2 and the DsRed reporter in pericytes and NG2-glia, and indicates that DsRed is more strongly expressed in pericytes, whereas NG2 immunolabeling picks up the true extent of the fine process fields of NG2-glia, which is less clear from DsRed expression. Scale bars = 20 μm in A, C, F, G, and 10 μm in B, D, E. [Color figure can be viewed in the online issue, which is available at www.interscience.wiley.com.]

NG2-glia are identified by expression of the red fluorescent protein DsRed (see Fig. 1). DsRed expression is a reliable marker for NG2-glia in these mice, but pericytes are also DsRed-positive, since they express the NG2 CSPG (Fig. 1, some indicated by curved arrows). To avoid any possibility of confusion with pericytes, calcium imaging was performed on NG2-glia located within the nerve parenchyma and not closely related to blood vessels (Fig. 1B, NG2-glia indicated by asterisks and pericytes by curved arrows). In addition, NG2-glia are readily distinguished from pericytes by their morphology and location within the nerve (Fig. 1C–E); pericytes have large soma directly apposed to blood vessels, whereas NG2-glia have small irregular somata, from which fine processes extend and branch two or more times, before terminating within approximately 20–30 μm of the cell body (Fig. 1C–E). Immunolabeling for NG2 in brain sections of NG2-DsRed BAC mice confirms co-expression of NG2 and the DsRed reporter in pericytes and NG2-glia (Fig. 1F,G). Confocal analysis of single z-sections of fluo-4 loaded nerves illustrates that DsRed-positive NG2-glia respond to glutamate (Fig. 2A–F, asterisks) and ATP (Fig. 4A–C, asterisks) by increases in $[Ca^{2+}]_i$; responding DsRed-negative glia were also observed in the same fields of view (Fig. 4A–C), and these are considered to be mostly astrocytes, although oligodendrocytes may also load with fluo-4 (Hamilton et al., 2008).

AMPA Receptors Mediate Ca^{2+} Signals in NG2-Glia

Confocal microscopic analysis of single z-sections shows that glutamate evokes raised $[Ca^{2+}]_i$ in DsRed-positive NG2-glia (Fig. 2A–F, asterisks). Patch-clamp studies have shown predominant AMPA-receptor induced currents in NG2-glia (Bergles et al., 2000; Kukley et al., 2007; Ziskin et al. 2007), and so we examined whether these mediate Ca^{2+} signals in NG2-glia, using cyclothiazide (CTZ, 10 μM), which blocks AMPA receptor desensitization, and NBQX (100 μM), an antagonist of AMPA-receptors (Fig. 2G,H). In paired recordings from DsRed-positive NG2-glia, fura-2 calcium imaging shows that the glutamate-induced Ca^{2+} increase was significantly increased by CTZ (to 245 ± 60% of the glutamate response in the same cells, $n = 8$; $P < 0.001$, Mann-Whitney; Fig. 2G,H). In a separate series of paired recordings from DsRed-positive NG2-glia, the glutamate response was significantly decreased by the AMPA-receptor antagonist NBQX (67 ± 4% of the glutamate response in the same cells $n = 21$; $P < 0.05$, Mann-Whitney; Fig. 2G,H). NBQX did not completely block the glutamate response in all NG2-glia, suggesting other glutamate receptors on NG2-glia. We therefore examined the response of NG2-glia to NMDA (100 μM) by fluo-4 confocal imaging of single z-sections in DsRed-positive NG2-glia (Fig. 3A–D). In an analysis of 54 cells from four nerves, we observed that NMDA evoked a rise in $[Ca^{2+}]_i$ in six cells (22%), and the amplitude of the response was very variable (Fig. 3A–D); however, we did not examine whether removal of Mg^{2+} or addition of glycine and/or D-serine increased the NMDA response in NG2-glia. Further analysis using fura-2 imaging in DsRed nerves showed that the NMDA induced Ca^{2+} increase was significantly decreased by the NMDA receptor antagonist D-AP5 (10 μM), to 44 + 6% ($n = 12$; $P < 0.001$, Mann-Whitney; Fig. 3E,F).

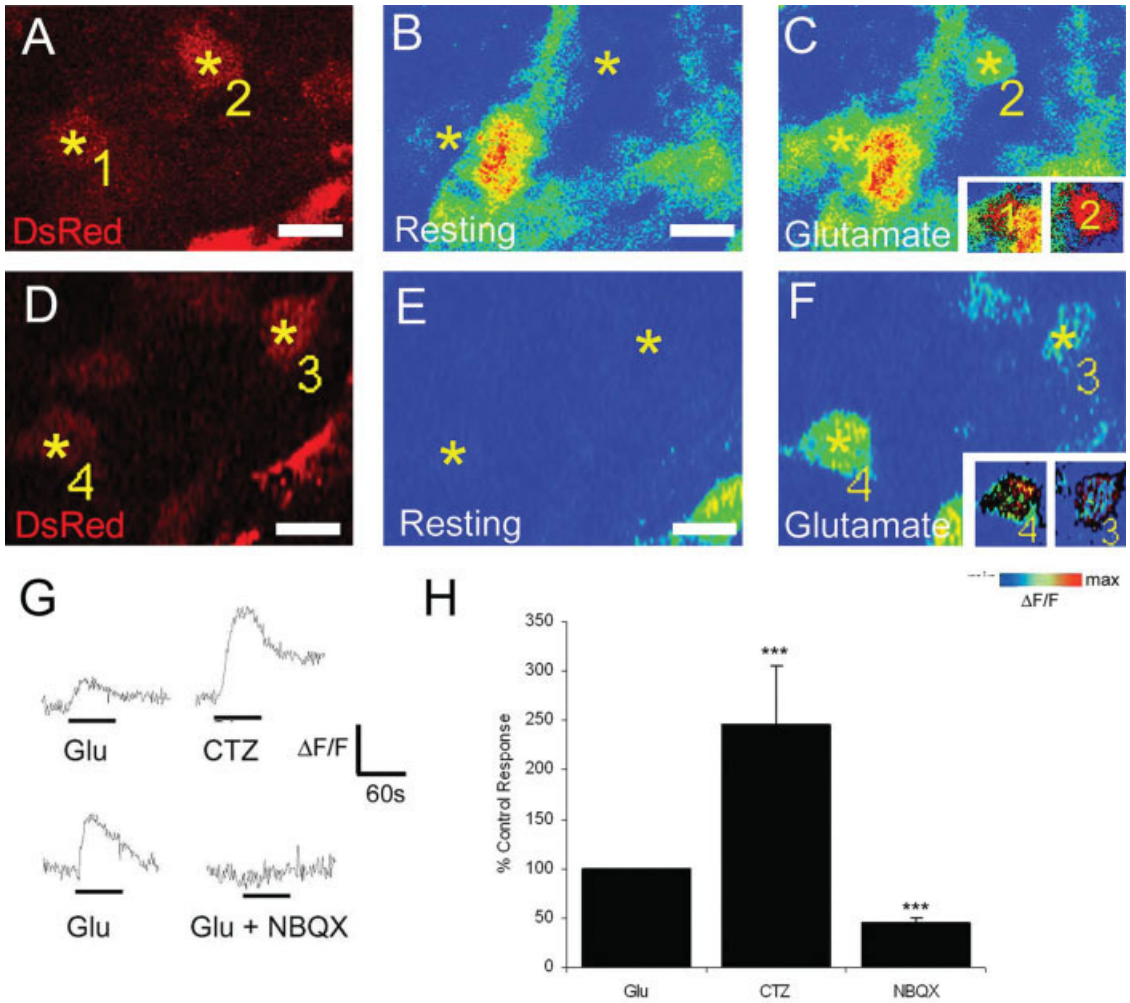

Fig. 2. Glutamate evoked responses in NG2-glia *in situ*. (**A–F**) Confocal micrographs of single z-sections of fluo-4 loaded nerves, illustrating NG2-glia identified by expression of DsRed in NG2-DsRed BAC mice (scale bars = 10 μm). NG2-glia respond to bath applied glutamate with a rise in $[Ca^{2+}]_i$ indicated by the increase in fluorescence (insets show DsRed channel superimposed on the fluo-4 channel). (**G**) Paired recordings from NG2-glia illustrating the typical response to bath application of 100 μM glutamate (60 s), and showing the actions of cyclothiazide (CTZ), which blocks AMPA receptor desensitization, and NBQX, an AMPA-receptor antagonist. (**H**) In paired recordings, the peak Ca^{2+} response to glutamate was significantly greater in CTZ (n = 8) and was significantly less in NBQX (n = 21). Data in (H) are means (±SEM) and are normalized as % of the glutamate response in the same cells (***$P < 0.001$, Mann-Whitney test). [Color figure can be viewed in the online issue, which is available at www.interscience.wiley.com.]

P2X and P2Y Purinoceptors Mediate Ca^{2+} Signals in NG2-Glia

Confocal calcium imaging of individual DsRed-positive NG2-glia in single z-planes demonstrates that ATP evokes a rapid and transient rise in $[Ca^{2+}]_i$ in these cells (Fig. 4A–C, asterisks). The predominant mechanism for ATP-mediated Ca^{2+} signaling in optic nerve glia is by metabotropic P2Y receptors, mainly of the $P2Y_1$ subtype, although glia express multiple subtypes of metabotropic P2Y and ionotropic P2X purinoceptors (James and Butt, 2002). We examined the actions of the $P2Y_1$ receptor preferring agonist 2MeSATP and the $P2Y_1$ antagonist MRS2179 (both at 100 μM; Fig. 4D), using fura-2 calcium imaging in P12-16 optic nerves from NG2/DsRed mice. In paired recordings of DsRed-positive NG2-glia, the response to 2MeSATP was not significantly different to ATP (107 ± 4% of the ATP response in the same cells, n = 40), and was significantly inhibited by MRS2179 (26 ± 5% of the 2MeSATP response in the same cells, n = 40; $P < 0.001$, ANOVA and Bonferroni test). In addition, there is a significant $P2X_7$ receptor mediated component of Ca^{2+} signaling in optic nerve glia (Hamilton et al., 2008), and so we examined whether these receptors are active in NG2-glia *in situ* (Fig. 4E). The potent $P2X_7$ receptor agonist BzATP produced a large increase in $[Ca^{2+}]_i$ in DsRed-positive NG2-glia, although significantly smaller than ATP (75 ± 4% of the ATP response in the same cells, n = 39; $P < 0.001$ ANOVA and Bonferroni test), and this was almost completely abolished by the $P2X_7$ antagonist oATP (9 ± 1% of the BzATP response in the same cells, n = 39; $P < 0.001$, ANOVA

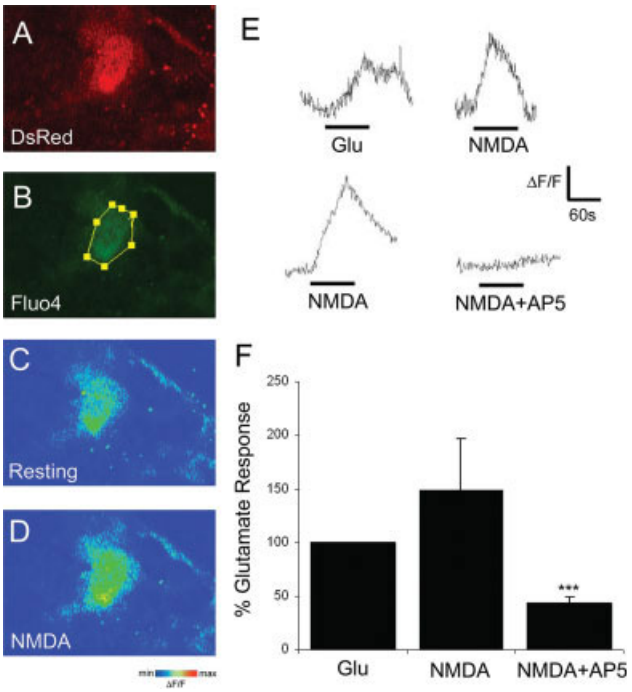

Fig. 3. NMDA evoked responses in NG2-glia *in situ*. (**A**–**D**) Confocal micrographs of single z-sections of fluo-4 loaded nerves, illustrating NG2-glia identified by expression of DsRed in NG2-DsRed BAC mice (scale bar = 10 μm). A small proportion of NG2-glia (6 out of 54 analyzed) responded to bath applied NMDA (100 μM) with a rise in $[Ca^{2+}]_i$. (**E**, **F**) Paired fura-2 recordings from NG2-glia, indicating that in cells that responded to NMDA, the response was similar to that evoked by glutamate (100 μM) and was significantly inhibited by AP-5 (n = 12). Data in (H) are means (±SEM) and are normalized as % of the glutamate response in the same cells (***$P < 0.001$, Mann-Whitney test). [Color figure can be viewed in the online issue, which is available at www.interscience.wiley.com.]

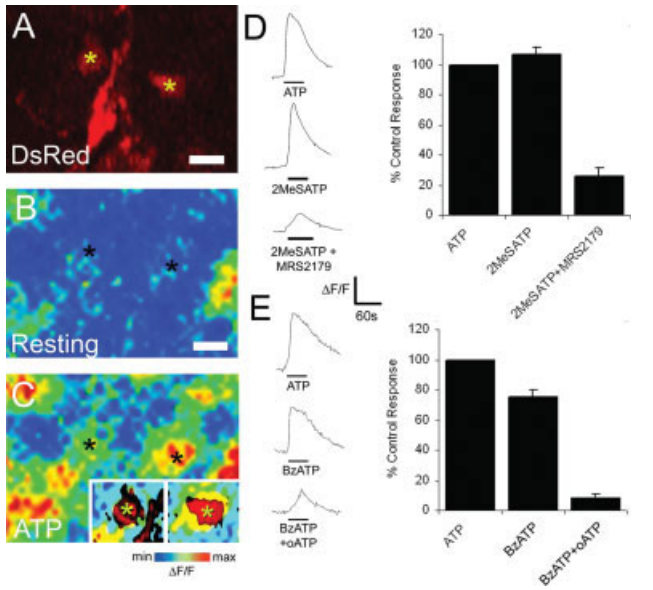

Fig. 4. Metabotropic and ionotropic purinergic (ATP) receptors mediate Ca^{2+} signals in optic nerve NG2-glia *in situ*. (**A**–**C**) Confocal micrographs of single z-sections of fluo-4 loaded nerves, illustrating NG2-glia identified by expression of DsRed in NG2-DsRed BAC mice (scale bars = 10 μm). NG2-glia respond to bath applied ATP with a rapid rise in $[Ca^{2+}]_i$ indicated by the increase in fluorescence (insets show DsRed channel superimposed on the fluo-4 channel). (**D**) In recordings from the same cells, the Ca^{2+} responses evoked by the P2Y agonist 2MeSATP were equivalent to ATP, and were significantly inhibited by the $P2Y_1$ receptor antagonist MRS2179 (n = 40). (**E**) Paired recordings show the $P2X_7$ receptor agonist BzATP (100 μM) evoked a large Ca^{2+} signal, and this was significantly inhibited by the P2 × 7 receptor antagonist oxidized ATP (oATP, n = 39). Data in (D) and (E) are means (±SEM) and are normalised as % of the ATP response in the same cells. ***$P < 0.001$, ANOVA followed by Bonferroni test. [Color figure can be viewed in the online issue, which is available at www.interscience.wiley.com.]

and Bonferroni test; Fig. 4E); BzATP may break down to adenosine, but the complete block by oATP indicates the Ca^{2+} response to BzATP is not due to stimulation of adenosine receptors. The results indicate significant roles for both $P2Y_1$ and $P2X_7$ receptors in mediating Ca^{2+} signals in NG2-glia.

ATP and Glutamate are Released During Axonal Electrical Activity to Evoke Ca^{2+} Signals in NG2-Glia

Confocal calcium imaging of individual DsRed-positive NG2-glia in single z-planes shows that electrical stimulation of nerves at 20 Hz for 10 s evoked Ca^{2+} signals in NG2-glia (Fig. 5A–F). The Ca^{2+} signals increased in both amplitude and duration with increasing stimulus strength (Fig. 5G; n = 7, $P < 0.001$, paired t-test), indicating a graduated response of NG2-glial Ca^{2+} signals that are matched to axonal activity. In addition, there was evidence of potentiation in some cells, whereby when two stimuli were applied sequentially the response to the second was greater than the first (Fig. 5H); this was not observed in all cases, and overall there was not significant difference in the mean response of two consecutive stimuli (n = 7; $P > 0.05$, paired t-test). The activity-dependent Ca^{2+} signal in NG2-glia (n = 29) was significantly decreased by the general P2 receptor antagonist suramin (10 μM), to 70 ± 8% ($P < 0.001$, Mann-Whitney test; Fig. 5I). Incubation of nerves in 100 μM NBQX did not significantly reduce the activity-dependent rise in $[Ca^{2+}]_i$ in any glia analysed (n = 64, response in NBQX was 107 ± 6% that in aCSF, $P > 0.05$, Mann-Whitney). However, incubation of nerves in TBOA and CTZ (to block glutamate uptake and block desensitization of AMPA receptors) resulted in a significant potentiation of Ca^{2+} signals in DsRed-positive NG2-glia (Fig. 5J), to 440 ± 229% of the 20 Hz response in aCSF in the same cells, n = 6; $P < 0.001$ ANOVAR and Bonferroni test), and this was significantly reduced by NBQX (239% of the 20 Hz response in aCSF in the same cells, n = 3; $P < 0.001$ ANOVAR and Bonferroni test). The effects of CTZ and TBOA reveal that glutamate released during axonal action potential propagation acts on AMPA-type receptors in NG2-glia, but without this pharmacological intervention, the role of glutamate in axon-to-NG2-glial cell Ca^{2+} excitability is minor compared with that of ATP.

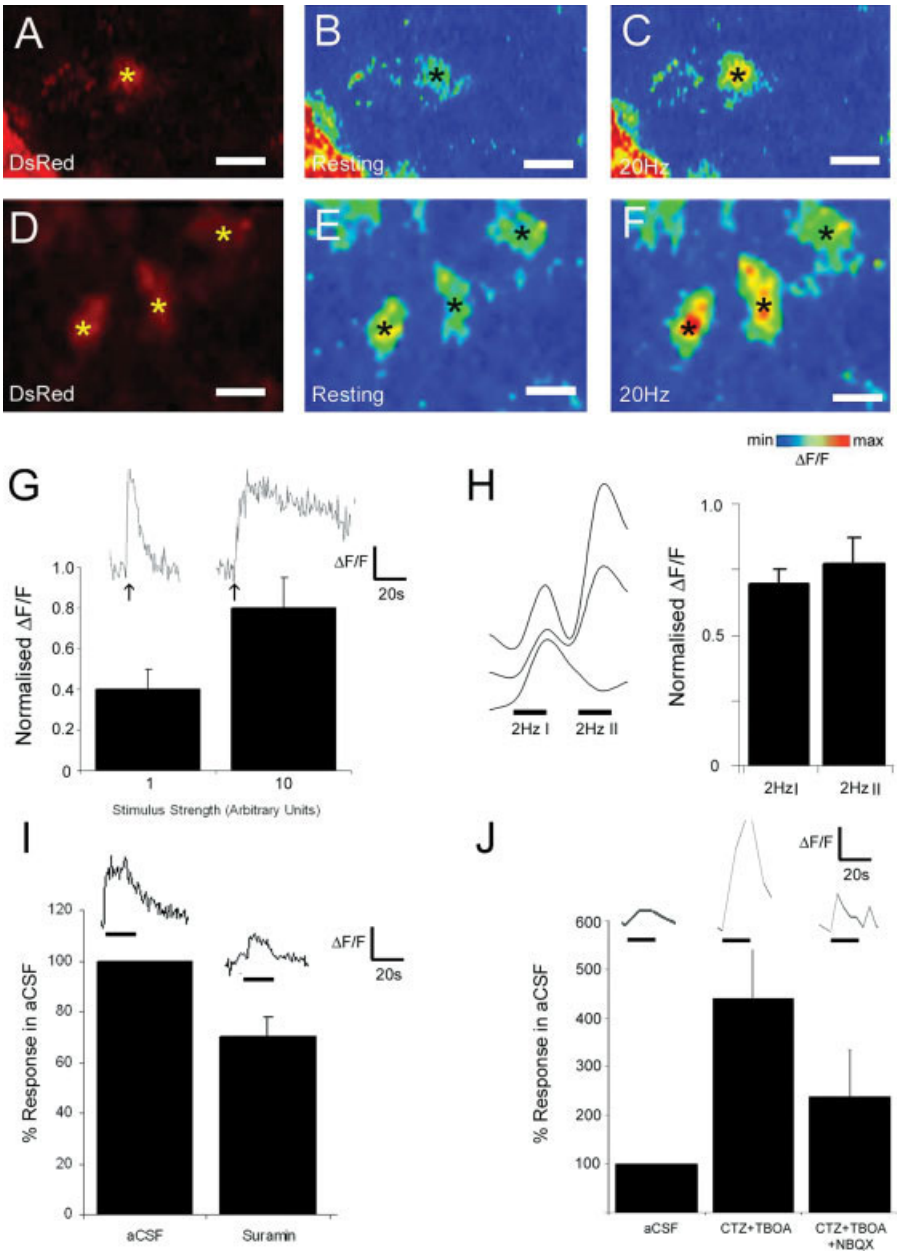

Fig. 5. Action potentials in white matter axons stimulate the release of ATP and glutamate and evoke Ca^{2+} signals in NG2-glia. (**A–F**) Confocal micrographs of single z-sections of fluo-4 loaded nerves, illustrating NG2-glia identified by expression of DsRed in NG2-DsRed BAC mice (scale bars = 10 μm). Axonal stimulation at 20 Hz for 10 s evoked a rise in $[Ca^{2+}]_i$ in NG2-glia (asterisks). (**G**) The size of the NG2-glial cell response increased with increasing stimulus strength ($n = 7$, $P < 0.001$, paired t-test); stimulus strength determines the number of axons firing action potentials, and indicates NG2-glial Ca^{2+} signals are matched to axonal activity. (**H**) Some NG2-glia displayed potentiation, where a second train of axonal action potentials resulted in an increased Ca^{2+} signal; this was not statistically different overall. (**I**) Action potential evoked Ca^{2+} signals in NG2-glia were significantly inhibited by the general P2 antagonist suramin (10 μM; $n = 29$). (**J**) Action potential evoked Ca^{2+} signals in NG2-glia were significantly augmented by cyclothiazide (CTZ) and TBOA ($n = 6$; $P < 0.001$ ANOVAR and Bonferroni test), and significantly inhibited by NBQX ($n = 3$; $P < 0.001$ ANOVAR and Bonferroni test). [Color figure can be viewed in the online issue, which is available at www.interscience.wiley.com.]

ATP Released by Astrocytes Evokes Ca^{2+} Signals in NG2-Glia

ATP has been shown to act as a "gliotransmitter" by optic nerve astrocytes (Hamilton et al., 2008), and so we examined intercellular Ca^{2+} signaling by fura-2 calcium imaging in NG2/DsRed nerves (see Fig. 6). Mechanical stimulation of the optic nerve with a microelectrode evoked an intercellular Ca^{2+} wave which initiated in DsRed-negative astrocytes and was transmitted to DsRed-positive NG2 -glia (Fig. 6A). Intercellular transmission of the Ca^{2+} signal was blocked by the general P2X/P2Y antagonist suramin (10 μm; Fig. 5B; response in suramin was 34 ± 11% of that in aCSF, $n = 37$, $P <$

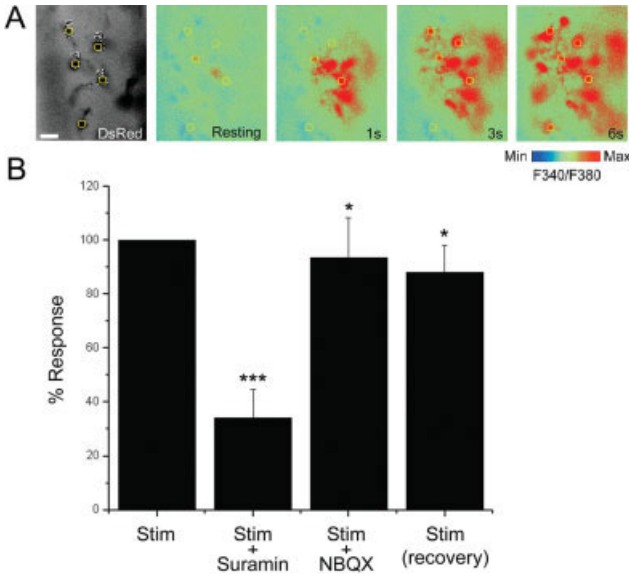

Fig. 6. Intercellular Ca^{2+} waves are transmitted to NG2-glia *in situ*. (**A**) Fura-2 calcium imaging in NG2/DsRed nerves illustrating that mechanical stimulation with a microelectrode evoked an intercellular Ca^{2+} wave that passed between DsRed-negative astrocytes and was transmitted to DsRed-positive NG2-glia. (**B**) The effects of P2 and AMPA receptor antagonists was examined in unidentified glia, and shows that the general purinoceptor antagonist suramin (10 μM; n = 37) significantly and markedly reduced the intercellular glial Ca^{2+} wave. The AMPA receptor antagonist NBQX (100 μM; n = 50) reduced the Ca2+ wave to a much smaller degree, but it was statistically significant. *$P < 0.05$, *** $P < 0.001$, Mann-Whitney test. [Color figure can be viewed in the online issue, which is available at www.interscience.wiley.com.]

0.001, Mann-Whitney test), whereas blockade of AMPA-type receptors with NBQX (100 μM) had a much smaller, but statistically significant effect (Fig. 6B; response in NBQX was 93 ± 15% of that in aCSF, n = 50, $P < 0.05$, Mann-Whitney test). The results indicate that mechanical stimulation stimulates the release of ATP, and to a smaller extent glutamate, which evoke Ca^{2+} signals that pass between astrocytes and NG2-glia.

Sites of Communication of NG2-Glia With Astrocytes and Axons

The results above provide evidence of axon-to-NG2-glia and astrocyte-to-NG2-glia signaling, and so we examined the points of communication between these elements (Figs. 7–9). Relations between astrocytes and NG2-glia were examined by NG2 immunolabeling of sections of optic nerve (Fig. 7A–C) and brain (Fig. 7D,E) from GFAP-GFP mice. The process domains of NG2-glia and astroglia overlap (Fig. 7A,D), and astrocytes form "en passant" contacts with the somata of NG2-glia (Fig. 7A), and *vice versa* (Fig. 7D). NG2-glial cell processes enwrapped short segments of astroglial processes (Fig. 7B,C), and in an equivalent manner astroglial processes enwrap segments of NG2-glial cell processes (Fig. 7E). In addition, we re-examined the relationship between NG2-glia and nodes of Ranvier, because although we have shown that NG2-glia contact nodes of Ranvier in the optic nerve (Butt et al., 1999), a subsequent study was unable to identify NG2-glial cell contacts with nodes of Ranvier in the corpus callosum, using NG2 immunolabeling or electron microscopy in the NG2-DsRed mouse (Ziskin et al., 2007). The true three-dimensional relations between axons and NG2-glia cannot be resolved in sections, and the use of mouse tissue severely restricts the possibilities of double and triple immunolabeling. We therefore used the rat anterior medullary velum (Figs. 8 and 9), where axon-glial relations can be clearly resolved in three dimensions (Butt and Berry, 2000). The axons examined in the P15 rat AMV will all ultimately be myelinated by P30, and at P15 we can examine the relations of NG2-glia with axons throughout the stages of myelination (Butt and Berry, 2000). NG2-glia distinctively sit apposed to axons and extend their processes along myelinated axons (Fig. 8A), premyelinated axons (Fig. 8B), and axons that are being actively myelinated (Fig. 9A,B). Double immunolabeling for NG2 and MBP to identify myelin sheaths shows that in myelinated axons, NG2-glia contact the myelin sheath at heminodes (Fig. 8Aii), and NG2-glial cell processes conjoin consecutive myelin sheaths and the nodal gap defined by the paranodes of the myelin sheaths (Fig. 8Aiii), suggestive of the NG2-glial process guiding the growing myelin sheaths to an identified point at the node. In premyelinated axons, double immunolabeling for NG2 and NF200 shows processes of NG2-glia bifurcate at the point of contact with axons (Figs. 8Bii, 8Biv), and spiral along the axon in both directions to partly circumnavigate short lengths of the axon (Fig. 8Biii), reminiscent of the initiating processes of premyelinating oligodendrocytes (Butt and Berry, 2000). Triple immunolabeling for NG2, MBP (myelin) and NF200 (axons) confirms that NG2-glia extend processes along the myelin sheath to form en passant contacts with axons at heminodes (Fig. 9A), as well as terminating on axons at developing nodes of Ranvier (Fig. 9B). This was examined further using triple immunolabeling for NG2, MBP, and ankyrinG, an axoskeletal protein that defines nodes of Ranvier (Lambert et al., 1997) (Fig. 9C). We analyzed raw confocal images, because image analysis programs using deconvolution and isoforming involve setting thresholds which, whilst providing a representation of the three-dimensional structure, significantly reduces the true extent of the immunolabeling by as much as 20%. Analysis of raw confocal images shows that in the anterior medullary velum individual NG2-glia contact many nodes of Ranvier within their domains, but not all nodes are contacted by NG2-glia (Fig. 9C); quantitative analysis indicated that in the velum 71 ± 8% of the nodes of Ranvier within a field of 50 μm^2 were contacted by NG2-glia (n = 7 cells). The majority of nodal contacts appear as en passant (Fig. 9D–F), and NG2-glial cell processes often passed close to nodes without appearing to contact them (Fig. 9G). Isoforming shows that some NG2-glial cell processes terminate at and partly ensheath the node of Ranvier (Fig. 9H), as we have shown previously (Butt et al., 1999, 2005).

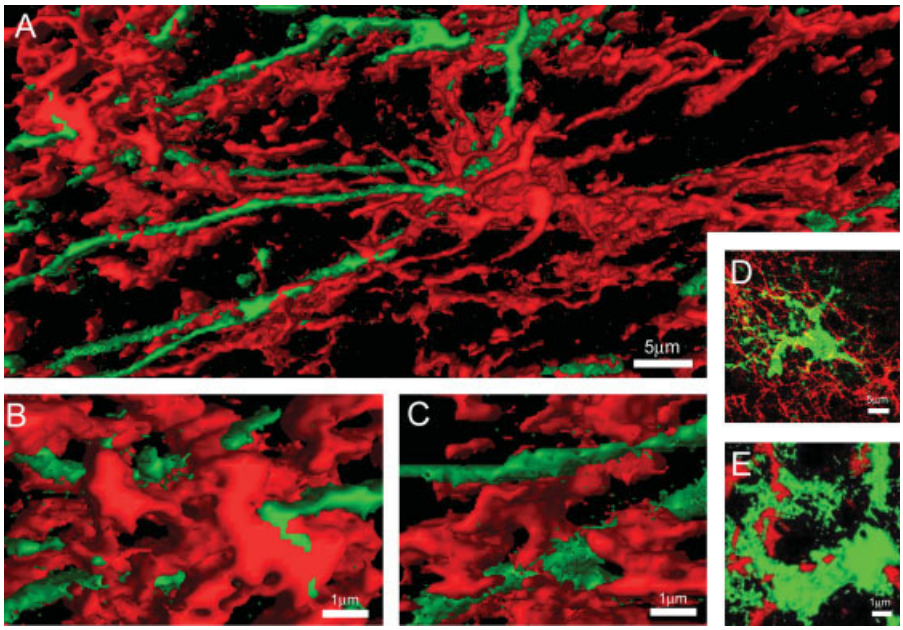

Fig. 7. Sites of communication between NG2-glia and astrocytes. Confocal microscopic examination of NG2 immunolabeling (red) and GFP+ astrocytes (green) in sections of P15 optic nerve (**A**–**C**) and cerebral cortex (**D**, **E**). (A–C) Three-dimensional isoformed reconstructions show astrocytes (green) form "en passant" associations with the somata of NG2-glia (red), and NG2-glial cell processes enwrap short lengths of astroglial processes. (D, E) Confocal micrographs in the cerebral cortex show the extent of the overlap of the process fields of astrocytes and NG2-glia, and isoformed reconstructions show that astrocyte processes enwrap short lengths of NG2-glial cell processes. [Color figure can be viewed in the online issue, which is available at www.interscience.wiley.com.]

Expression of Glutamate Receptors and Synaptophysin by NG2-Glia

The results presented above provide functional evidence of AMPA-type and NMDA-type glutamate receptors in NG2-glia. We examined this using an antibody against GluR4 and an antibody that recognizes both NR2A and NR2C subunits (NR2AC), in addition to an antibody against the synaptic protein synaptophysin (Fig. 10). We performed immunolabeling on sections from DsRed mice aged P15 to allow visualization of NG2-glia without double immunolabeling, which would have been complicated by the possibility of cross-reactivity because the NG2, GluR4, and NR2AC are rabbit antibodies. Images were analyzed by confocal microscopy and using Volocity software to calculate overlap coefficients in three-dimensions. Three-dimensional images were captured as z-stacks, and are illustrated as two-dimensional flattened images of single channels of the DsRed-positive NG2-glia (Fig. 10Ai,Bi,Ci), immunolabeling for GluR4 (Fig. 10Aii), synaptophysin (Fig. 10Bii) and NR2AC (Fig. 10Cii), and the two channels combined (Fig. 10Aiii,Biii,Ciii). Colocalization channels were generated to illustrate the voxels from the two channels that overlap with equal intensity (Fig. 10Aiv,Biv,Civ); these are two-dimensional representations of the true extent of colocalization of the two channels in three-dimensions. Figures 10D,E illustrate single z-sections (central panels), together with 90° rotations illustrating

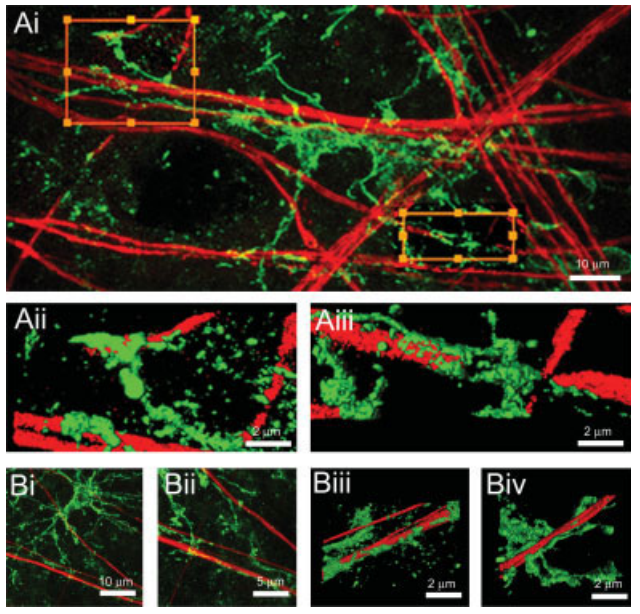

Fig. 8. Sites of communication between NG2-glia and axons. Confocal microscopic examination of double immunofluorescence labeling for NG2 (green) and myelin basic protein (red, **A**) or neurofilament-200 (red, **B**) in whole-mounts of anterior medullary velum from P15 rats. (A) NG2-glial cell with soma directly apposed to axons (Ai) and extending processes along myelinated axons to terminate at the paranodal myelin sheath of a heminode (Aii), and to conjoin consecutive myelin sheath paranodes and almost fill the nodal gap (Aiii). (B) Relations of a NG2-glial cell and premyelinated axons (Bi), illustrating NG2-glial cell processes bifurcating at the point of contact with an axon (Bii), and partly ensheathing short lengths of axons (Biii, iv). [Color figure can be viewed in the online issue, which is available at www.interscience.wiley.com.]

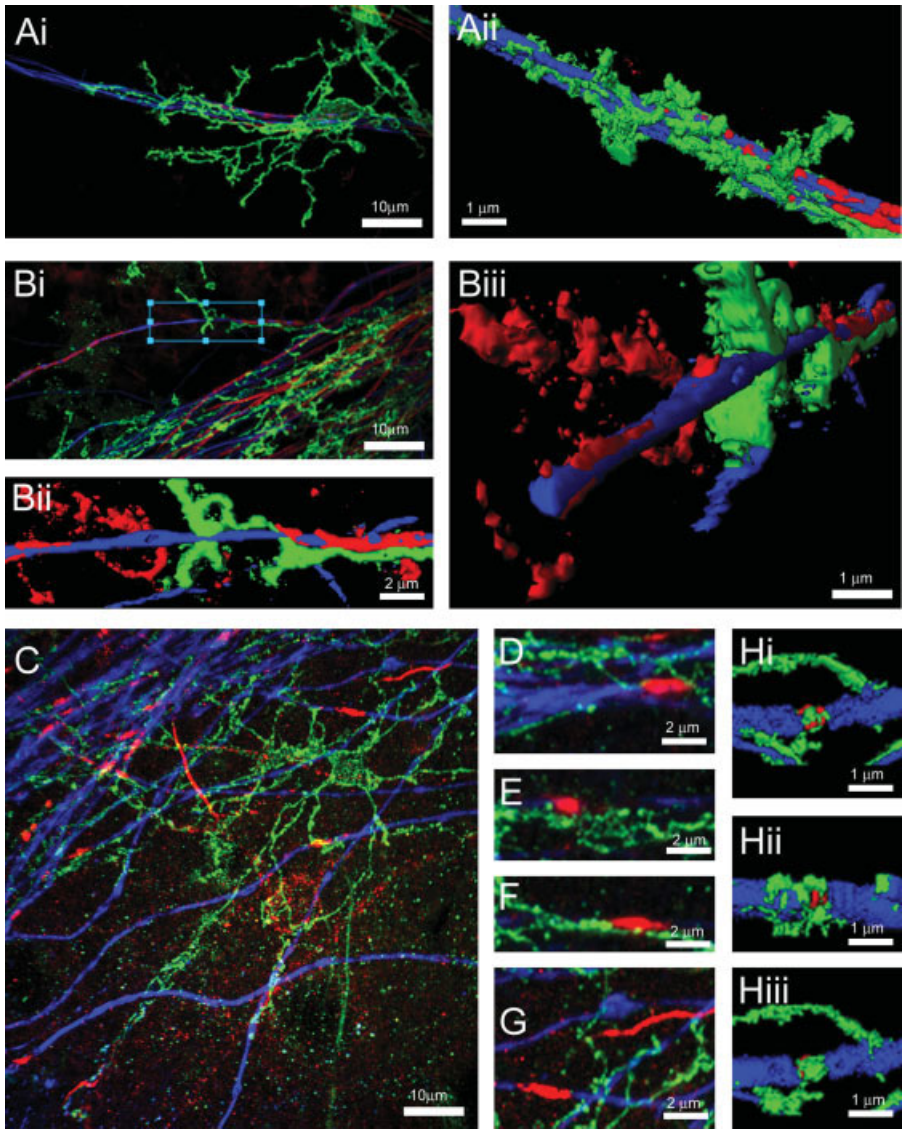

Fig. 9. Association of NG2-glia with nodes of Ranvier. Confocal microscopic and three-dimensional isoformed reconstructions in whole-mounts of P15 rat anterior medullary vela. (**A**, **B**) Triple immunolabeling for NG2 (green), MBP (red) and NF200 (blue) show NG2-glial cells with soma directly apposed to axons that are in the process of being actively myelinated. (A) NG2-glial cell extending a process along the myelin sheath of a heminode and terminates along the premyelinated axon segment (Aii). (B) NG2-glial cell sitting along a bundle of axons extends a process to follow one myelinated segment and terminate at a developing node of Ranvier, characterized by a large nodal gap and loosely wrapped paranodal myelin sheaths (Bii). (**C**–**H**) Triple immunolabeling for NG2 (green), MBP (blue) and ankyrinG (red), an axoskeletal protein that defines nodes of Ranvier (Lambert et al., 1997). (C) NG2-glial cell forming close associations with many, but not all, nodes of Ranvier within its domain. (D–G) Raw confocal images of nodes of Ranvier, showing en passant nodal associations of NG2-glia (D–F), and NG2-glial cell process passing close to nodes without contacting them (G). (H) Three-dimensional isoformed reconstruction of an NG2-glial cell process that terminates at a node of Ranvier and partly ensheaths the axon. [Color figure can be viewed in the online issue, which is available at www.interscience.wiley.com.]

transects through the cell body in the *x-x* plane (top panels) and *y-y* plane (left-hand panels), and a representation of voxels through 360° in the *x-y-z* planes (corner panels). The overlap coefficient was calculated as a measure of this colocalization of the signals from the two channels in voxels throughout the three-dimensional image (Fig. 10F); it is important to note that each voxel in each z-section is examined to determine where the two channels overlap with equal intensity, and so the overlap coefficient is not simply a measurement of overlap from the two-dimensional flattened images illustrated in Figures 10A–C. The results indicate that coexpression of GluR4 and synaptophysin are greater than NR2AC, but suggest all three are expressed in the cell bodies and primary processes of NG2-glia (Fig. 10Aiv, Biv,Civ). There is clear evidence for cellular expression of synaptophysin (Fig. 10D) and GluR4 (Fig. 10E) in DsRed-positive NG2-glia (coexpression appears as yellow), and colocalization analysis ($n = 10$ cells in each case) demonstrates significantly ($P < 0.05$, unpaired *t*-test) higher overlap coefficients for GluR4 (0.61 ± 0.02) and synaptophysin (0.59 ± 0.01) than for NR2AC (0.53 ± 0.01). An overlap coefficient of <0.5 indicates there is little true colocalization, and this was the case in 4 out

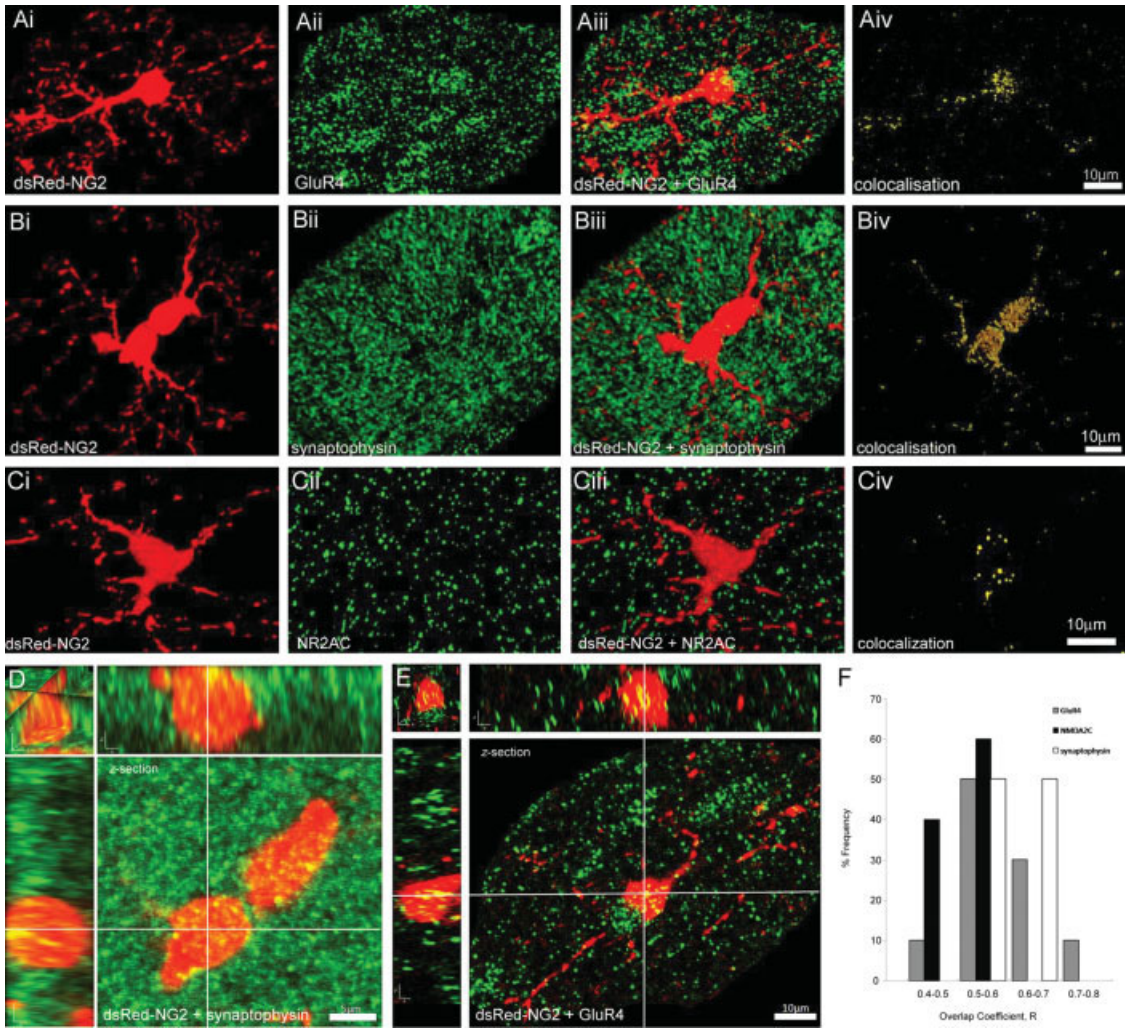

Fig. 10. Expression of synaptic proteins by NG2-glia. Confocal examination of cortical sections from P15 NG2-dsRed transgenic mice immunolabeled for the GluR4 of the AMPA receptor (**A**, **E**), the synaptic protein synaptophysin (**B**, **D**), and the NR2A and 2C subunits of the NMDA receptor (**C**). Single channels for NG2 (Ai, Bi, Ci), GluR4 (Aii), synaptophysin (Bii), and NR2AC (Cii), combined channels (Aiii, Biii, Ciii), and analysis showing the extent of colocalization of GluR4 (Aiv), synaptophysin (Biv) and NR2A (Civ) on NG2-glial cell somata and processes. (D, E) There was widespread immunolabeling for GluR4 and synaptophysin, but the three-dimensional voxel analysis in single z-sections (D and E main panels), the *x-y-z* plane (D and E top left), the z-transect in the *x* plane (D and E, top right panels), and z-transect in the *y* plane (C and D, left panels), indicates GluR4 and synaptophsysin immunolabeling within the cell somata of NG2-glia. (**F**) Graphic representation of the overlap coefficients for DsRed with GluR4, NR2AC, and synaptophysin, determined by three-dimensional analysis of voxels using Volocity software. The results indicate lower expression of NR2AC than GluR4 and synaptophysin in NG2-glia ($n = 10$ cells for each). It is important to note that the overlap coefficient is a measure of the degree of colocalization of the two channels in voxels and not in pixels; each voxel is examined through 360°, as illustrated by the three-dimensional rotations and transects illustrated in (D) and (E), and it is not simply a measurement of overlap from the two-dimensional images illustrated in (A–C). [Color figure can be viewed in the online issue, which is available at www.interscience.wiley.com.]

of 10 NG2-glia analyzed for NR2AC, for only 1 out of 10 NG2-glia analyzed for GluR4, and none of the 10 cells analyzed for synaptophysin (Fig. 10F). For further comparison, we also analyzed expression of the vesicular glutamate transporter VGLUT1 in NG2-glia, and found overlap coefficients of ≤ 5 (mean of 0.42 ± 0.05, $n = 10$), indicating NG2-glia do not express VGLUT1 (not illustrated). The results indicate greater expression of GluR4 and synaptophysin than NR2AC in NG2-glia, and there is also evidence of expression of GluR4 and synaptophysin in the fine processes of NG2-glia (Fig. 10Aiv,Biv), but this was less clear for NR2AC (Fig. 10Civ).

DISCUSSION

Astroglia use intercellular Ca^{2+} waves as a mechanism for communication (Verkhratsky et al., 1998). Here, we provide evidence of Ca^{2+} excitability in NG2-glia. Activation of AMPA-type glutamate receptors and $P2Y_1$ and $P2X_7$ purine receptors evoke Ca^{2+} signals in NG2-glia. The results also supported the possibility that NG2-glia express functional NMDA receptors, but the evidence was not strong. Mechanisms for vesicular release of glutamate have been shown at nodes of Ranvier in optic nerve axons (Alix et al., 2008), and we show

here that NG2-glia contact nodes of Ranvier and sense glutamate released during action potential propagation. In addition, we show that astroglial release of ATP following mechanical stimulation evokes Ca^{2+} signals in NG2-glia, and we identify the sites of communication between astrocytes and NG2-glia as distinctive en passant contacts that their processes form on each others somata, and as bipartite ensheathment of short segments of each others processes. Notably, we also observed expression of AMPA receptors and the synaptic protein synaptophysin in NG2-glial cell somata and processes, suggesting that NG2-glia may be capable of bidirectional communication with astrocytes and axons. However, unless glutamate uptake and AMPA-receptor desensitization are blocked, the glutamate released during action potential propagation evokes only small Ca^{2+} signals in NG2-glia, suggesting Ca^{2+} influx is not the predominant mechanism of action of glutamate on NG2-glia. In contrast, ATP released by astrocytes and during action potential propagation evokes a large Ca^{2+} signal in NG2-glia. The results indicate a potential multiphase axon-glial mechanism, in which glutamate released by electrically active axons is sensed by NG2-glia, but does not ordinarily evoke a large Ca^{2+} signal, and the main mechanism for Ca^{2+} signaling in NG2-glia is via ATP released by astrocytes in response to axonal activity.

AMPA Receptors Mediate Ca^{2+} Signaling to NG2-Glia

Activation of AMPA-type receptors mediated glutamate-evoked Ca^{2+} signals in optic nerve NG2-glia, suggestive of AMPA receptors lacking the GluR2 subunit which confers a higher Ca^{2+} permeability (Matute et al., 1997). This is supported by studies in the optic nerve that detected all of the GluR subunits with the exception of GluR2 (Jensen and Chiu, 1993; Salter and Fern, 2005). The small Ca^{2+} signal evoked by glutamate in NG2-glia is consistent with rapid opening and closing of AMPA receptors, which recover between 30 and 500 ms (Krampfl et al., 2002). The marked increase in the Ca^{2+} signal in the presence of TBOA and cyclothiazide demonstrates that the response to glutamate is dampened by glutamate uptake and receptor desensitization. This would serve to reduce the possibility of excitotoxic Ca^{2+} influx, to which OPCs have been shown to be particularly sensitive (Fern and Möller, 2000; Matute et al., 2005). In addition, there is evidence of functional NMDA receptors in NG2-positive OPCs in brain slices (Karadottir et al., 2005), and these have been shown to mediate raised Ca^{2+} in OPCs in culture (Wang et al., 1996). We observed that NMDA mediated raised Ca^{2+} in NG2/DsRed-glia *in situ*, but this was observed in only 22% of cells. We did not examine whether removal of Mg^{2+} or addition of glycine and/or D-serine increased the NMDA response in NG2-glia, but this did not alter the response in optic nerve astrocytes (Hamilton et al., 2008), suggesting that endogenous levels of glycine and/or D-serine are sufficient to co-activate NMDA-R in the optic nerve, and NMDA-R in glia do not appear to display a large Mg^{2+} block (Karadottir et al., 2005; Lalo et al., 2006). NMDA receptor subunits NR1, NR2, and NR3 have been demonstrated in the optic nerve (Micu et al., 2005; Salter and Fern, 2005), and using an antibody that recognizes the NR2A and 2C receptor subunits, we provide evidence of NMDA receptor expression in NG2-glia. However, the level of expression was not strong, and colocalization analysis indicated a lower overlap coefficient than for GluR4. The increased glutamate-induced Ca^{2+} influx in the presence of cyclothiazide, which blocks the desensitization of AMPA-Rs, and the fact that this was blocked by NBQX, indicates that a large proportion of glutamate-induced Ca^{2+} elevation in NG2-glia is mediated by Ca^{2+} permeable AMPA-R. However, activation of AMPA-R may also result in depolarization and Ca^{2+} entry through voltage-operated calcium channels and the residual glutamate-mediated Ca^{2+} elevation in the presence of NBQX suggest Ca^{2+} influx may also occur through metabotropic GluR.

A Dominant Role for ATP in Ca^{2+} Signaling in NG2-Glia

The ATP-evoked Ca^{2+} signals in NG2-glia were mediated by both metabotropic $P2Y_1$ and ionotropic $P2X_7$ receptors, and were generally more rapid and larger than those observed in response to glutamate. Although NG2-glia had not been studied in this context previously, $P2Y_1$ and $P2X_7$ receptors have been demonstrated in OPC's (Agresti et al., 2005; Wang et al., 2008). Our results suggest that $P2Y_1$ receptors generate the characteristic transient Ca^{2+} signal resulting from the release of Ca^{2+} from intracellular stores in NG2-glia, and the Ca^{2+} response evoked by BzATP and its blockade by oATP is evidence of $P2X_7$ receptors on NG2-glia in situ (Hamilton et al., 2008; Wang et al., 2009). $P2Y_1$ receptors may have a greater role in physiological signaling, since they are activated at nanomolar concentrations of ATP in optic nerve glia, whereas $P2X_7$ receptors are generally activated when extracellular ATP reaches micromolar levels, and may therefore be more important in pathology (Agresti et al., 2005; James and Butt, 2001; Matute et al., 2007; Wang et al. 2009). Nonetheless, extracellular ATP has been shown to reach 78 μM following stimulation of the retina (Newman, 2001), and in the present study the glial Ca^{2+} signals evoked by release of ATP following mechanical and electrical stimulation in the optic nerve were equivalent to those evoked by exogenous application of 100 μM ATP, suggesting this level is within physiological limits. Hence, $P2X_7$ and $P2Y_1$ receptors would both be activated by ATP released by axons and astrocytes. Low levels of ATP would activate the transient self-limiting $P2Y_1$ receptor-mediated release of Ca^{2+} from intracellular stores, whereas at higher levels of signaling, Ca^{2+} influx through $P2X_7$ receptors would serve to prolongs the ATP-evoked Ca^{2+} signal for hundreds of seconds. This would provide a mechanism for the temporal coding of activity-dependent Ca^{2+} signals in NG2-glia and requires further investigation.

Axonal Activity Stimulates Ca^{2+} Signaling in NG2-Glia

The NG2-glial response to axonal stimulation was inhibited by the general P2X/P2Y antagonist suramin, whereas blockade of AMPA receptors was not effective unless the glutamate response was augmented by TBOA and CTZ. Some NG2-glia also displayed potentiation of the Ca^{2+} signal in response to axonal electrical activity, which is similar to hippocampal NG2-glia, where activation of Ca^{2+}-permeable AMPA receptors has been shown to mediate a form of activity-dependent "long-term potentiation" (Ge et al., 2006). Myelinated and nonmyelinated axons have mechanisms for vesicular glutamate release (Alix et al., 2008; Ziskin et al., 2007), and vesicular release of glutamate by axons has been demonstrated to act directly on AMPA receptors in NG2-glia (Ziskin et al., 2007). We found that NG2-glial express GluR4 subunits of the AMPA receptor on their cell bodies and processes, and show that NG2-glial cell somata lie on axons and their processes extend along premyelinated axons and contact myelinated axons at nodes of Ranvier. However, in the present study, axonal release of glutamate only evoked Ca^{2+} signals in NG2-glia when uptake was blocked and AMPA receptor desensitization was blocked with cyclothiazide. It seems likely that axonal action potentials mediate highly localized rapid neuron-glial signaling events, which either do not normally result in significant Ca^{2+} influx, or result in brief and/or highly localized rises in $[Ca^{2+}]_i$ which were not resolved in our study. In contrast, perfusion of glutamate will activate AMPA-Rs on both processes and somata, and the finding that perfusion mediates a larger rise in Ca^{2+} than axonal activity is consistent with our immunohistochemical observation that GluR4 appear to be more prevalent on the cell bodies and primary processes of NG2-glia. Our results show that axonal activity does not result in a rise in Ca^{2+} via these GluR, indicating they are activated physiologically by glial sources of glutamate, and that they may play an important role in pathological spillover of glutamate. In contrast, our results indicate ATP released during action potential propagation mediates a much larger Ca^{2+} signal. The release of ATP by axons has been shown to evoke Ca^{2+} signals in OPCs co-cultured with neurons within seconds of evoking action potentials (Stevens et al., 2002). Optic nerve axons may also release ATP, but we have shown that axonal action potentials stimulate astroglial release of ATP as a "gliotransmitter" in the optic nerve (Hamilton et al., 2008), and this may be the main Ca^{2+} signaling input onto NG2-glia.

ATP Released by Astrocytes Stimulates Ca^{2+} Signaling in NG2-Glia

The propagation of intercellular Ca^{2+} waves between astrocytes and NG2-glia demonstrated in the present study involved mainly ATP, although the actions of NBQX indicate that glutamate was also released. Astroglial release of ATP has been demonstrated extensively in numerous preparations (Coco et al., 2003; Newman, 2001), and this involves multiple mechanisms, including release through vesicles, reversed transport, hemichannels, volume-sensitive anion channels, and $P2X_7$ receptors (Parpura et al., 2004). In optic nerve astrocytes, ATP release involves $P2X_7$ receptors, since intercellular signaling is reduced in $P2X_7$ knock-out mice and when $P2X_7$ receptors are pharmacologically blocked (Hamilton et al., 2008). The present study provides the first evidence that astroglial intercellular signaling is transmitted to NG2-glia, indicating that astrocytes can modulate the function of NG2-glia, much in the same way that they release neurotransmitters and modulate synaptic efficacy in neurons (Fiacco and McCarthy, 2006). Moreover, we provide evidence that NG2-glia express synaptophysin, indicating they may be capable of neurotransmitter release and bidirectional communication with astrocytes. Some NG2-glia also displayed potentiation of the Ca^{2+} signal in response to axonal electrical activity, which is similar to hippocampal NG2-glia, where activation of Ca^{2+}-permeable AMPA receptors has been shown to mediate a form of activity-dependent "long-term potentiation" (Ge et al., 2006). Our finding that NG2-glia may also express synaptic proteins supports the suggestion of Ge and colleagues (2006) that Ca^{2+}-dependent secretion of neuroactive factors from NG2-glia would allow rapid feedback regulation of axonal (neuronal) functions and that the strength of this feedback would increase after the induction of potentiation, which they termed gLTP (Ge et al., 2006).

CONCLUSIONS

Our results show that ATP and glutamate are active signaling molecules in the optic nerve and mediate Ca^{2+} excitability in NG2-glia. Glutamate and ATP are important in regulating the development of OPCs and axonal myelination (Agresti et al., 2005; Stevens et al., 2002; Wang et al., 1996; Yuan et al., 1998). Oligodendrocyte generation in the optic nerve is largely complete at the ages used in the present study (Greenwood and Butt, 2003). However, some NG2-expressing glia maintain an OPC function after myelination is complete (Rivers et al., 2008), and so signaling from axons and astrocytes may regulate these cells, which would also have importance for remyelination in the demyelinating disease, multiple sclerosis. The present study provides clear evidence of a physiological role for ATP in Ca^{2+} signaling in NG2-glia. In contrast, bath applied glutamate evoked Ca^{2+} signals in NG2-glia, whereas glutamate released during axonal action potential propagation did not. The effects of TBOA indicate that glutamate released by axons is effectively cleared and spill-over to activate receptors on NG2-glial cell somata is not significant, since this would have evoked a robust Ca^{2+} signal similar to that seen when glutamate was bathed over the nerve. The latter may mimic pathology, when extracellular levels of glutamate and ATP are high and activation

of AMPA and $P2X_7$ receptors could mediate gliosis or cytotoxicity in NG2-glia, which is relevant to numerous pathologies, including physical trauma, multiple sclerosis, stroke, and cerebral palsy (Hamilton et al., 2009; Matute et al., 2005, 2007; Wang et al., 2009). In contrast, physiological glutamate and ATP signaling may be highly localized and transmitted via processes contacting axons and astrocytes. In conclusion, the expression of multiple receptors with different sensitivities and kinetics provides NG2-glia with a mechanism for a graduated response to axonal and astroglial signals. Moreover, evidence that NG2-glia express the synaptic protein synaptophysin suggests that they may also be capable of vesicular release and bidirectional communication with astrocytes and axons via their cellular contacts.

ACKNOWLEDGMENTS

The authors thank Merdol Ibrahim for some of the confocal images, and David Attwell for comments on the manuscript.

REFERENCES

Agresti ME, Meomartini S, Amadio E, Ambrosini C, Volonte F, Aloisi S, Visentin S. 2005. ATP regulates oligodendrocyte progenitor migration, proliferation, and differentiation: Involvement of metabotropic P2 receptors. Brain Res Brain Res Rev 48:157–165.

Alix JJ, Dolphin AC, Fern R. 2008. Vesicular apparatus, including functional calcium channels, are present in developing rodent optic nerve axons and are required for normal node of Ranvier formation. J Physiol 586:4069–4089.

Bergles DE, Roberts JD, Somogyi P, Jahr CE. 2000. Glutamatergic synapses on oligodendrocyte precursor cells in the hippocampus. Nature 405:187–191.

Bolton S, Butt AM. 2005. The optic nerve: A model for axon-glial interactions. J Pharmacol Toxicol Methods 51:221–233.

Butt AM, Berry M. 2000. Oligodendrocytes and the control of myelination in vivo: New insights from the rat anterior medullary velum. J Neurosci Res 59:477–488.

Butt AM, Duncan A, Hornby MF, Kirvell SL, Hunter A, Levine JM, Berry M. 1999. Cells expressing the NG2 antigen contact nodes of Ranvier in adult CNS white matter. Glia 26:84–91.

Butt AM, Hamilton N, Hubbard P, Pugh M, Ibrahim M. 2005. Synantocytes: The fifth element. J Anat 207:695–706.

Butt AM, Kiff J, Hubbard P, Berry M. 2002. Synantocytes: New functions for novel NG2 expressing glia. J Neurocytol 31:551–565.

Coco S, Calegari F, Pravettoni E, Pozzi D, Taverna E, Rosa P, Matteoli M, Verderio C. 2003. Storage and release of ATP from astrocytes in culture. J Biol Chem 278:1354–1362.

Fern R, Möller T. 2000. Rapid ischemic cell death in immature oligodendrocytes: a fatal glutamate release feedback loop. J Neurosci 20:34–42.

Fiacco TA, McCarthy KD. 2006. Astrocyte calcium elevations: properties, propagation, and effects on brain signaling. Glia 54:676–690.

Ge WP, Yang XJ, Zhang Z, Wang HK, Shen W, Deng QD, Duan S. 2006. Long-term potentiation of neuron-glia synapses mediated by Ca2+-permeable AMPA receptors. Science 312:1533–1537.

Greenwood K, Butt AM. 2003. Evidence that perinatal and adult NG2-glia are not conventional oligodendrocyte progenitors and do not depend on axons for their survival. Mol Cell Neurosci 23:544–558.

Hamilton N, Vayro S, Kirchhoff F, Verkhratsky A, Robbins J, Gorecki D, Butt AM. 2008. Mechanisms of ATP- and glutamate-mediated calcium signaling in white matter astrocytes. Glia 56:734–749.

Hamilton N, Hubbard P, Butt AM. 2009. Effects of glutamate receptor activation on NG2-glia in the rat optic nerve. J Anat 214:208–219.

James G, Butt AM. 2001. P2X and P2Y purinoreceptors mediate ATP-evoked calcium signalling in optic nerve glia in situ. Cell Calcium 30:251–259.

James G, Butt AM. 2002. P2Y and P2X purinoceptor mediated Ca^{2+} signalling in glial cell pathology in the central nervous system. Eur J Pharmacol 447:247–260.

Jensen AM, Chiu SY. 1993. Expression of glutamate receptor genes in white matter: Developing and adult rat optic nerve. J Neurosci 13:1664–1675.

Karadottir R, Cavelier P, Bergersen LH, Attwell D. 2005. NMDA receptors are expressed in oligodendrocytes and activated by ischaemia. Nature 438:1162–1166.

Krampfl K, Schlesinger F, Zorner A, Kappler M, Dengler R, Bufler J. 2002. Control of kinetic properties of GluR2 flop AMPA-type channels: Impact of R/G nuclear editing. Eur J Neurosci 15:51–62.

Kriegler S, Chiu SY. 1993. Calcium signalling of glial cells along mammalian axons. J Neurosci 13:4229–4245.

Kukley M, Capetillo-Zarate E, Dietrich D. 2007. Vesicular glutamate release from axons in white matter. Nat Neurosci 10:311–320.

Lalo U, Pankratov Y, Kirchhoff F, North RA, Verkhratsky A. 2006. NMDA receptors mediate neuron-to-glia signaling in mouse cortical astrocytes. J Neurosci 26:2673–2683.

Lambert S, Davis JQ, Bennett V. 1997. Morphogenesis of the node of Ranvier: Co-clusters of ankyrin and ankyrin-binding integral proteins to define early developmental intermediates. J Neurosci 17:7025–7036.

Lin SC, Huck JH, Roberts JD, Macklin WB, Somogyi P, Bergles DE. 2005. Climbing fiber innervation of NG2-expressing glia in the mammalian cerebellum. Neuron 46:773–785.

Newman EA. 2001. Propagation of intercellular calcium waves in retinal astrocytes and Muller cells. J Neurosci 21:2215–2223.

Matute C, Alberdi E, Domercq M, Sánchez-Gómez MV, Pérez-Samartín A, Rodríguez-Antigüedad A, Pérez-Cerdá F. 2007. Excitotoxic damage to white matter. J Anat 210:693–702.

Matute C, Domercq M, Sanchez-Gomez M-V. 2005. Glutamate-mediated glial injury: Mechanisms and clinical importance. Glia 53:212–224.

Matute C, Sanchez-Gomez MV, Martinez-Millan L, Miledi R. 1997. Glutamate receptor mediated toxicity in optic nerve oligodendrocytes. Proc Natl Acad Sci USA 94:8830–8835.

Micu I, Jiang Q, Coderre E, Ridsdale A, Zhang L, Woulfe J, Yin X, Trapp BD, McRory JE, Rehak R, Zamponi GW, Wang W, Stys PK. 2006. NMDA receptors mediate calcium accumulation in myelin during chemical ischaemia. Nature 439:988–992.

Nolte C, Matyash M, Pivneva T, Schipke CG, Ohlemeyer C, Hanisch UK, Kirchhoff F, Kettenmann H. 2001. GFAP promoter-controlled EGFP-expressing transgenic mice: A tool to visualize astrocytes and astrogliosis in living brain tissue. Glia 33:72–86.

Parpura V, Scemes E, Spray DC. 2004. Mechanisms of glutamate release from astrocytes: Gap junction "hemichannels", purinergic receptors and exocytotic release. Neurochem Int 45:259–264.

Rivers LE, Young KM, Rizzi M, Jamen F, Psachoulia K, Wade A, Kessaris N, Richardson WD. 2008. PDGFRA/NG2 glia generate myelinating oligodendrocytes and piriform projection neurons in adult mice. Nat Neurosci 11:1392–1401.

Salter MG, Fern R. 2005. NMDA receptors are expressed in developing oligodendrocyte processes and mediate injury. Nature 438:1167–1171.

Stevens B, Porta S, Haak LL, Gallo V, Fields RD. 2002. Adenosine: A neuron-glial transmitter promoting myelination in the CNS in response to action potentials. Neuron 36:855–868.

Verkhratsky A, Orkand RK, Kettenmann H. 1998. Glial calcium: Homeostasis and signalling function. Physiol Rev 78:99–141.

Wang LY, Cai WQ, Chen PH, Deng QY, Zhao CM. 2009. Downregulation of P2X7 receptor expression in rat oligodendrocyte precursor cells after hypoxia ischemia. Glia 57:307–319.

Wang C, Pralong WF, Schulz MF, Rougon G, Aubry JM, Pagliusi S, Robert A, Kiss JZ. 1996. Functional *N*-methyl-D-aspartate receptors in O-2A glial precursor cells: a critical role in regulating polysialic acid-neural cell adhesion molecule expression and cell migration. J Cell Biol 135:1565–1581.

Wigley R, Hamilton N, Nishiyama A, Kirchhoff F, Butt AM. 2007. Morphological and physiological interactions of NG2-glia with astrocytes and neurons. J Anat 210:661–670.

Yuan X, Eisen AM, McBain CJ, Gallo V. 1998. A role for glutamate and its receptors in the regulation of oligodendrocyte development in cerebellar tissue slices. Development 125:2901–2914.

Zhu X, Bergles E, Nishiyama A. 2008. NG2 cells generate both oligodendrocytes and gray matter astrocytes. Development 135:145–157.

Zinchuk V, Zinchik O, Okada T. 2007. Quantitative colocalization analysis of multicolour confocal immunofluorescence microscopy images: Pushing pixels to explore biological phenomena. Acta Histochem Cytochem 40:101–111.

Ziskin JL, Nishiyama A, Rubio M, Fukaya M, Bergles DE. 2007. Vesicular release of glutamate from unmyelinated axons in white matter. Nat Neurosci 10:321–30.